ISOTHERMS, THERMODYNAMICS AND KINETICS OF RHODAMINE B DYE ADSORPTION ON NATURAL DIATOMITE

Pham Dinh Du

Thu Dau Mot University

ABSTRACT

In this paper, Phu Yen diatomite was used as adsorbent for adsorption rhodamine B (RB) dye in aqueous solution. Analysis methods, including SEM, XRD, FT-IR, and N_2 adsorption-desorption isotherms, were used to characterise the adsorbent. The analysis of experimental adsorption data showed that the adsorption followed Langmuir isotherm model and pseudo-second-order kinetic equation. Based on the adsorption constant in the Langmuir isotherm (K_L), thermodynamic parameters (ΔG^o, ΔH^o and ΔS^o) for adsorption of RB onto the diatomite were calculated. The results indicated that the process is spontaneous and endothermic in nature.

Keywords: *diatomite, rhodamine B, adsorption.*

1. INTRODUCTION

The removal of coloured and colourless organic pollutants from industrial wastewater is considered an important application of adsorption processes using a suitable. There is growing interest in using low cost, commercial available materials for the adsorption of dyes. Diatomite is a material that can satisfy these conditions.

Diatomite is a sedimentary rock primarily composed of the skeletons of microscopic single celled aquatic plants called diatoms. It consists of a wide variety of shapes and characterized by a high porosity up to 80%, low density and high surface area [1]. These properties show that its is a potential adsorbent for pollutants found in industrial wastewater including dyes [1].

The aim of this work is to examine the effectiveness of local diatomaceous earth for the removal of rhodamine B dye from aqueous solution. The morphology, structure and porosity properties of the diatomite were investigated.

2. EXPERIMENTAL

2.1. Adsorbent and methods for material analysis

Diatomite was obtained from Phu Yen provine, Vietnam. The samples were washed with distilled water to remove fines and other adhered impurities, filtered, dried at 100^{o}C, denoted as PYD. Scanning electron microscopy (IMS-NKL) analysis was carried out for PYD to study the development of morphology. The crystalline structure was obtained on

VNU-D8 Advance Instrument (Bruker, Germany) using Cu Kα radiation with λ = 1.5418 Å, over the range of 2θ = 10–70°. N_2 adsorption-desorption isotherms at 77K were measured using a Micromeritics Tristar 3000 equipment. Fourier transform infrared (FT-IR) spectra of the sample was measured on a Jasco FT/IR-4600 spectrometer (Japan) with a range of 500-4000 cm^{-1}.

2.2. Adsorbate and adsorption studies

The cationic dye, rhodamine B (denoted as RB) (HiMedia, India), was used as adsorbate (chemical structure shown in Fig. 1a).

Adsorption kinetics and isotherm experiments for the samples were undertaken in a batch reactor with 250 mL capacity provided with water circulation arrangement to maintain the temperature at desired value. Adsorption of the dyes performed by shaking 0.02 g of PYD in 100 mL of solution with varying concentrations at 30 and 45°C. The samples were collected by separation of PYD from solution using a centrifuge. UV-Vis absorption spectra were recorded by an UVD-3000 (Labomed, USA). Concentration of dye was determined spectrophotometrically by measuring absorbance at 554 nm for λ_{max} of RB (Fig. 1b). The data obtained from the adsorption studies were used to calculate the adsorption capacity, q_t (mol/g), of the adsorbent by a mass-balance relationship, which represents the amount of adsorbed dye per amount of the dry adsorbent:

$$q_t = \frac{(C_o - C_t).V}{m} \qquad (1)$$

where C_o and C_t are concentrations of the dyes in solution (mol/L) at time t = 0 and t = t, respectively. V is the volume of the solution (L), and m is weight of the dry adsorbent (g).

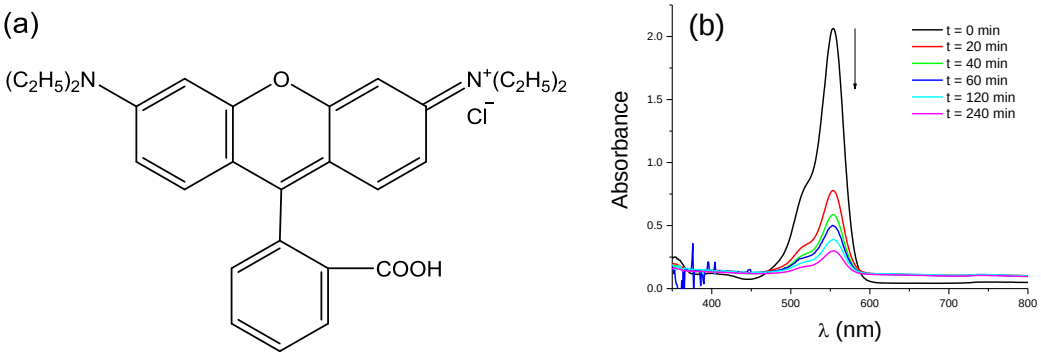

Fig. 1. *(a) Chemical structure for rhodamine B (RB); (b) UV-Vis absorption spectra for aqueous solutions of RB along with PYD in various adsorption times at 30°C (adsorbent dosage 0.2 $g.L^{-1}$, initial RB concentration 2.09 × 10^{-5} $mol.L^{-1}$)*

3. RESULTS AND DISCUSSION

3.1. Characterization of diatomite

The morphology and crystallographic information of PYD were characterized by SEM and XRD, and shown in Fig. 2. The SEM of PYD in Fig. 2(a) showed that the structure of diatomite was circular cylinder. There were many small holes on the surface. The XRD pattern (Fig. 2(b)) shows reflections which are typical for amorphous silica (a broad

reflection centered at $2\theta = 20 - 25^o$) and crystallized quartz (reflection peak centered nearly at $2\theta = 27^o$) [2]. Thus, the received diatomite consists of mainly amorphous structure.

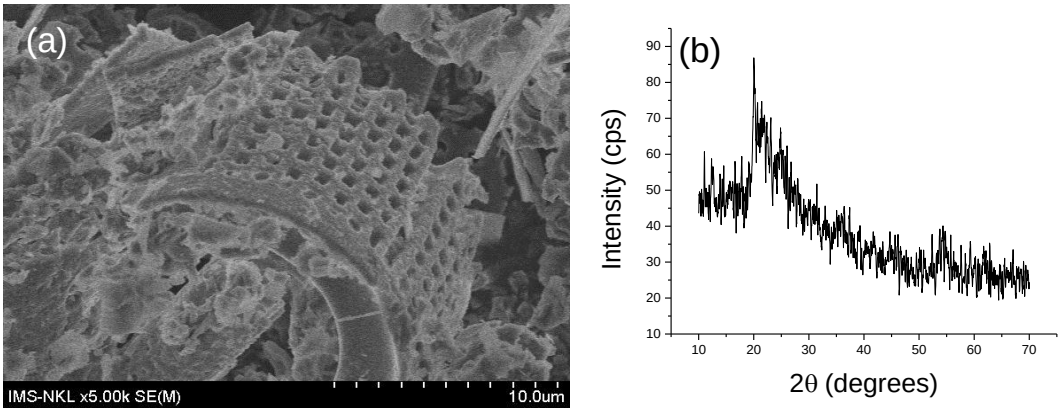

Fig. 2. *(a) SEM image and (b) XRD pattern of diatomite*

The FT-IR spectra of the PYD is shown in Fig. 3(a). It can be seen that there were four main absorption bands at 3392, 1613, 1031, and 784 cm^{-1}. The broad band around 3392 cm^{-1} represents the O–H stretching of the interlayer water molecules and framework hydroxyl groups, while the weak band at 1613 cm^{-1} is probably due to the bending vibrations of O–H groups of the adsorbed water molecules. The absorption peak at 1031 cm^{-1} reflected stretching vibration mode of Si–O–Si bond in the diatomite. The absorption peak at 784 cm^{-1} was attributed to the Si–O–Al bond, which was induced by the impurity ingredients of the clay in the original diatomite [1, 3].

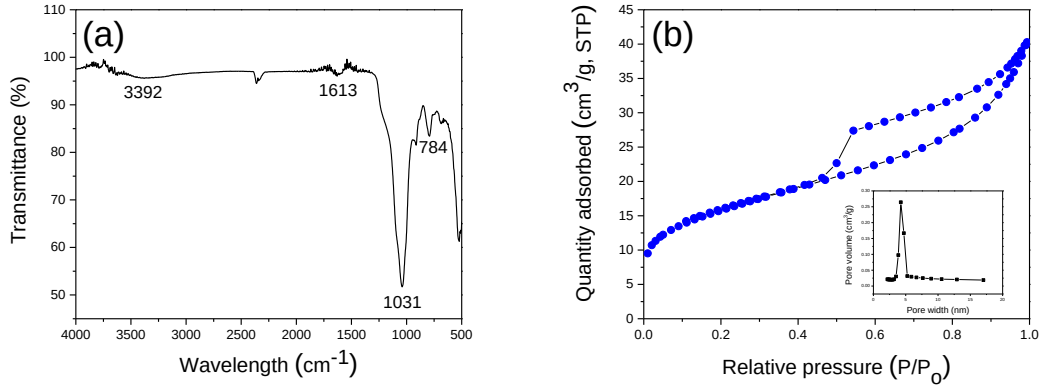

Fig. 3. *(a) FT-IR spectra and (b) N_2 adsorption-desorption isotherms of diatomite*

Fig. 3(b) shows the N_2 adsorption-desorption isotherms and pore-size distribution of the PYD. The diatomite exhibited a type II isotherm and a H3-type hysteresis loop, indicating the presence of macroporous structure with nonuniform size and/or shape [4]. Thus, the morphologies of the PYD consisted of variety of shapes (Fig. 2(a)). However, the pore-size distribution curves in the inset of Fig. 3(b) demonstrated an uniform of pore size distribution with an average diameter of 4.2 nm. According to the Brunauer-Emmett-Teller analysis, the PYD exhibits large specific surface area of 55.4 m^2/g, which is much higher than those of the diatomite in previous work [1, 3].

3.2. Adsorption isotherms and adsorption thermodynamics

In isotherm study, two commonly used models, the Freundlich [5, 6] and Langmuir [5, 6, 7] isotherms were applied to understand the dye-adsorbent interaction. The Freundlich isotherm is an empirical equation that assumes that the adsorption surface becomes heterogeneous during the course of the adsorption process. The heterogeneity arises form the presence of different functional groups on the surface and from the various adsorbent-adsorbate interactions. The Freundlich isotherm is expressed by the following empirical equation:

$$q_e = K_F C_e^{1/n} \quad (2)$$

In logarithmic form, Eq. (2) can be represented as:

$$\log q_e = \log K_F + \frac{1}{n} \log C_e \quad (3)$$

where q_e is the amount of RB adsorbed per unit of adsorbent at equilibrium (mol/g), C_e is the concentration of the dye solution at equilibrium (mol/L), K_F and n are Freundlich adsorption isotherm constants, which indicate the extent of the adsorption and the degree of nonlinearity between the solution concentration and the adsorption, respectively. The values of K_F and n can be calculated from the intercept and slope of the linear plot between logC_e and logq_e and are listed in Table 1. In general, as the K_F value increases, the adsorption capacity of the adsorbent for a given adsorbate also increases. The value of the Freundlich exponent n is in the range of $n > 1$, indicating that the adsorption process is favorable [5, 6].

The Langmuir adsorption model is based on the assumption that the maximum adsorption corresponds to a saturated monolayer of solute molecules on the adsorbent surface. The equation is given as:

$$q_e = \frac{q_m K_L C_e}{1 + K_L C_e} \quad (4)$$

The linear form of Eq. (4) can be described by:

$$\frac{C_e}{q_e} = \frac{1}{q_m K_L} + \frac{C_e}{q_m} \quad (5)$$

where C_e is the concentration of dye solution at equilibrium (mol/L), q_e is the amount of RB adsorbed per unit of adsorbent at equilibrium (mol/g), q_m is the maximum amount of adsorption with complete monolayer coverage on the adsorbent surface (mol/g), and K_L is the Langmuir constant, which is related to the energy of adsorption (L/mol). The Langmuir constants K_L and q_m can be determined form the intercept and slope of the linear plot of C_e/q_e versus C_e (Fig. 4) and are presented in Table 1.

The essential characteristics of the Langmuir isotherm can be expressed in terms of a dimensionless constant separation factor R_L [6], which is given by Eq. (6):

$$R_L = \frac{1}{1 + K_L C_o} \quad (6)$$

where C_o (mol/L) is the highest initial concentration of adsorbate, and K_L (L/mol) is the Langmuir constant. The parameter R_L indicates the nature of shape of the isotherm accordingly:

$R_L > 1$	Unfavorable adsorption
$0 < R_L < 1$	Favorable adsorption
$R_L = 0$	Irreversible adsorption
$R_L = 1$	Linear adsorption

Table 1 shows that the value of R_L is 0.0467 and 0.0332 at 30^{o}C and 45^{o}C, respectively, indicating that the adsorption of RB on PYD is favorable at the temperature studied. The R^2 values of the Langmuir isotherm are higher than Freundlich isotherm, indicating that the equilibrium sorption data fits best with the Langmuir isotherm. This data confirms that the adsorption of RB on PYD occurs as a monolayer coverage process. The maximum adsorption capacities (q_m) of RB on PYD are 2.20×10^{-4} and 1.93×10^{-4} (mol/g) at 30^{o}C and 45^{o}C, respectively.

Table 1. *Isotherm parameters for adsorption of RB dye onto the diatomite*

Temperature (^{o}C)	Freundlich			Langmuir			
	n	K_F	R^2	q_m (mol/g)	K_L (L/mol)	R^2	R_L
30	2.8003	0.0080	0.9738	2.20×10^{-4}	2.45×10^5	0.9880	0.0467
45	2.9682	0.0061	0.9104	1.93×10^{-4}	3.49×10^5	0.9955	0.0332

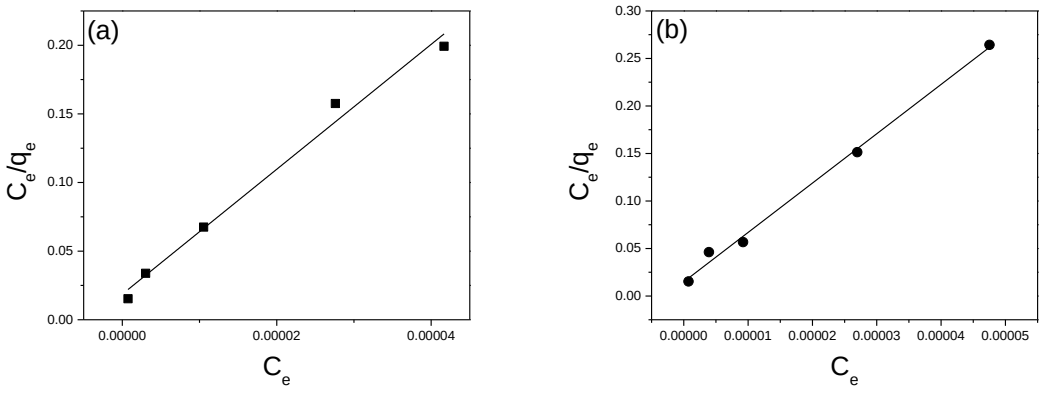

Fig. 4. *Langmuir plots for adsorption of RB onto the diatomite at 30^{o}C (a) and 45^{o}C (b)*

Based on the adsorption constant in the Langmuir isotherm (K_L), thermodynamic parameters (ΔG^o, ΔH^o and ΔS^o) for adsorption of RB onto PYD were calculated using Eqs. (7) – (9) [5, 7] and the results were given in Table 2. In Eq. (8), K_{L1} and K_{L2} are adsorption constant at T_1 and T_2.

$$\Delta G^o = -RT\ln K_L \quad (7)$$

$$\Delta H^o = -R\left(\frac{T_2 T_1}{T_2 - T_1}\right)\ln\frac{K_{L1}}{K_{L2}} \quad (8)$$

$$\Delta S^o = \frac{\Delta H^o - \Delta G^o}{T} \quad (9)$$

As can be seen, the adsorption process is spontaneous with the negative value of ΔG^o. As shown Table 2, the decreased value of ΔG^o from –31.26 kJ/mol (30^{o}C) to –33.74 kJ/mol (45^{o}C) indicated increased adsorption with increase in temperature. The standard enthalpy

change (ΔH^o) for adsorption of the dyes on PYD is positive, indicating that the process is endothermic in nature with ΔH^o of 18.90 kJ/mol. The positive value of ΔS^o suggeste increased randomness at the solid/solution interface occur in the internal structure of the adsorption of RB dye onto the diatomite.

Table 2. Thermodynamic parameters for adsorption of RB dye onto the diatomite

Temperature (^{o}C)	ΔG^o (kJ.mol^{-1})	ΔH^o (kJ.mol^{-1})	ΔS^o (J.mol^{-1}.K^{-1})
30	–31.26	18.90	165.53
45	–33.74		

3.3. Adsorption kinetics

Adsorption kinetic models were used to acquire a better understanding of the mechanism by which the dye is adsorbed from aqueous solutions by the diatomite. In this study, two models were used to investigate the details of the RB adsorption process onto PYD: the Lagergren pseudo-first-order model, and the Ho pseudo-second-order model [5, 6, 7].

The Lagergren pseudo-first-order model is based on the assumption that the rate of change of solute uptake over time is directly proportional to the difference in saturation concentration and the amount of solid uptake over time:

$$\frac{dq_t}{dt} = k_1(q_e - q_t) \qquad (10)$$

Intergrating Eq. (10) and noting that $q_t = 0$ at $t = 0$ gave following equation:

$$ln(q_e - q_t) = ln(q_e) - k_1 t \qquad (11)$$

where q_t is the amount of dye adsorbed per unit of adsorbent (mol/g) at time t, k_1 is the pseudo-first-order rate constant (min^{-1}), and t is the contact time (min). The adsorption rate constant (k_1) and the theoretical q_e values ($q_{e,cal}$) were calculated from the plot of ln($q_e - q_t$) versus t (Table 3).

Table 3. *Pseudo-first-order kinetic parameters for different initial RB dye concentrations at 30^{o}C and 45^{o}C*

$C_o \times 10^5$ (mol/L)	30^{o}C				45^{o}C			
	$q_{e,exp} \times 10^5$ (mol/g)	$q_{e,cal} \times 10^5$ (mol/g)	k_1 (min^{-1})	R^2	$q_{e,exp} \times 10^5$ (mol/g)	$q_{e,cal} \times 10^5$ (mol/g)	k_1 (min^{-1})	R^2
1.04	4.85	0.75	0.0159	0.9205	4.85	0.96	0.0174	0.9268
2.09	8.93	3.08	0.0164	0.9829	8.48	2.03	0.0179	0.9445
4.18	15.6	5.53	0.0131	0.9560	16.3	5.10	0.0162	0.9738
6.26	17.5	6.29	0.0164	0.9933	17.8	6.07	0.0169	0.9767
8.35	20.9	6.47	0.0048	0.7325	18.0	5.79	0.0203	0.9157

The Ho pseudo-second-order model is presented as:

$$\frac{dq_t}{dt} = k_2(q_e - q_t)^2 \qquad (12)$$

and when $q_t = 0$ at $t = 0$, Eq. (12) can be integrated into following equation:

$$\frac{t}{q_t} = \frac{1}{k_2 q_e^2} + \frac{t}{q_e} \qquad (13)$$

where k_2 is the pseudo-second-order rate constant (g.mol^{-1}.min^{-1}).

The initial adsorption rate, h (mol.g^{-1}.min^{-1}), at t = 0 is defined as:

$$h = k_2 q_e^2 \qquad (14)$$

The values of h, q_e and k_2 can be obtained from the linear plot of t/q_t versus t (Fig. 5). The kinetic parameters obtained from the pseudo-second-order model for adsorption of the dye are given in Table 4. The highest values of R^2 were observed with the pseudo-second-order model, and the theoretical $q_{e,cal}$ values obtained from this model were also closer to the experimental $q_{e,exp}$ values at different initial RB concentrations. These results indicate that the pseudo-second-order kinetic model gave a better correlation for the adsorption of RB on PYD compared to the pseudo-first-order model.

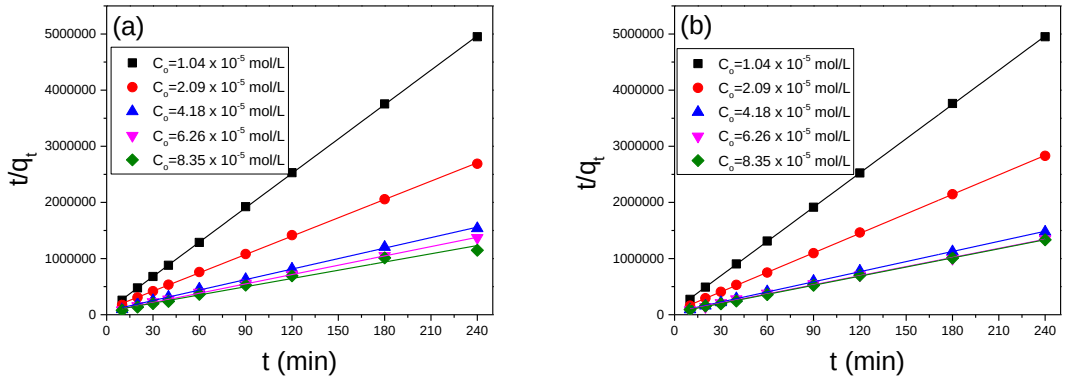

Fig. 5. *Pseudo-second-order kinetics for adsorption of RB dye onto PYD at 30°C (a) and 45°C (b)*

Table 4. *Pseudo-second-order kinetic parameters for different initial RB dye concentrations at 30°C and 45°C*

$C_o \times 10^5$ (mol/L)	30°C				45°C			
	$q_{e,exp} \times 10^5$ (mol/g)	$q_{e,cal} \times 10^5$ (mol/g)	k_2 (g/mol min)	R^2	$q_{e,exp} \times 10^5$ (mol/g)	$q_{e,cal} \times 10^5$ (mol/g)	k_2 (g/mol min)	R^2
1.04	4.85	4.89	6168.2	0.9999	4.85	4.92	4872.8	1.0000
2.09	8.93	9.18	1272.7	0.9997	8.48	8.64	2242.2	0.9999
4.18	15.6	16.1	594.0	0.9987	16.3	16.6	795.0	0.9995
6.26	17.5	18.1	601.8	0.9992	17.8	18.5	629.0	0.9990
8.35	20.9	20.5	406.7	0.9857	18.0	18.5	785.9	0.9997

The initial adsorption rate, h, for C_o = 8.35 × 10^{-5} mol/L at 45°C was 2.68 × 10^{-5} mol.g^{-1}.min^{-1} while for C_o = 1.04 × 10^{-5} mol/L the initial rate was only 1.18 × 10^{-5} mol.g^{-1}.min^{-1}. This could be due to the greater concentration gradient between the solid and liquid phase at the higher dye concentration. The maximum initial sorption rates were 1.96 × 10^{-5} mol.g^{-1}.min^{-1} (C_o = 6.26 × 10^{-5} mol/L) and 2.68 × 10^{-5} mol.g^{-1}.min^{-1} (C_o = 8.35 × 10^{-5} mol/L) at 30°C and 45°C, respectively.

4. CONCLUSION

In summary, the diatomite showed high surface area and amorphous structure. The adsorption of rhodamine B onto diatomite followed the pseudo-second order kinetic model

and the Langmuir isotherm model. The maximum adsorption capacities are 2.20×10^{-4} and 1.93×10^{-4} (mol/g) at 30°C and 45°C, respectively. The positive ΔH^o and negative ΔG^o for the adsorption process confirm the endothermic nature of the adsorption and spontaneous.

REFERENCES

[1] M. A. M. Khraisheh, Y. S. Al-degs, W. A. M. Mcminn, Remediation of wastewater containing heavy metals using raw and modified diatomite, Chem. Eng. J. 99 (2004) 177–184.

[2] J. Jin, J. Ouyang, H. Yang, One-step synthesis of highly ordered Pt/MCM-41 from natural diatomite and the superior capacity in hydrogen storage, Appl. Clay Sci. 99 (2014) 246–253.

[3] Y. Du, G. Zheng, J. Wang, L. Wang, J. Wu, H. Dai, MnO_2 nanowires in situ grown on diatomite: Highly efficient adsorbents for the removal of Cr(VI) and As (V), Micropor. Mesopor. Mat. 200 (2014) 27–34.

[4] G. Leofanti, M. Padovan, G. Tozzola, B. Venturelli, Surface area and pore texture of catalysts, Catalysis Today 41 (1998) 207-219.

[5] S. Sohrabnezhad, A. Pourahmad, Comparison absorption of new methylene blue dye in zeolite and nanocrystal zeolite, Desalination 256 (2010) 84–89.

[6] A. A. Jalil, S. Triwahyono, S. H. Adam, N. D. Rahim, M. A. A. Aziz, N. H. H. Hairom, N. A. M. Razali, M. A. Z. Abidin, M. K. A. Mohamadiah, Adsorption of methyl orange form aqueous solution onto calcined Lapindo volcanic mud, J. Hazard. Mater. 181 (2010) 755–762.

[7] S. Eftekhari, A. Habibi-Yangjeh, Sh. Sohrabnezhad, Application of AlMCM-41 for competitive adsorption of methylene blue and rhodamine B: Thermodynakic and kinetic studies, J. Hazard. Mater. 178 (2010) 349–355.

Article history:

– Received: Apr. 19.2016

– Accepted: Aug. 20.2016

– Email: dupd@tdmu.edu.vn